Primary cilia dynamics instruct tissue patterning and repair of corneal endothelium

Andrea L. Blitzer[a], Lampros Panagis[b,1], G. Luca Gusella[c], John Danias[b,1], Marek Mlodzik[a,2], and Carlo Iomini[a,2]

Departments of [a]Developmental and Regenerative Biology, [b]Ophthalmology, and [c]Medicine, Mount Sinai School of Medicine, New York, NY 10029

Edited* by Kathryn V. Anderson, Sloan-Kettering Institute, New York, NY, and approved January 11, 2011 (received for review November 10, 2010)

Primary cilia are required for several signaling pathways, but their function in cellular morphogenesis is poorly understood. Here we show that emergence of an hexagonal cellular pattern during development of the corneal endothelium (CE), a monolayer of neural crest-derived cells that maintains corneal transparency, depends on a precise temporal control of assembly of primary cilia that subsequently disassemble in adult corneal endothelial cells (CECs). However, cilia reassembly occurs rapidly in response to an in vivo mechanical injury and precedes basal body polarization and cellular elongation in mature CECs neighboring the wound. In contrast, CE from hypomorphic *IFT88* mutants (*Tg737*^{orpk}) or following in vivo lentiviral-mediated IFT88 knockdown display dysfunctional cilia and show disorganized patterning, mislocalization of junctional markers, and accumulation of cytoplasmic acetylated tubulin. Our results indicate an active role of cilia in orchestrating coordinated morphogenesis of CECs during development and repair and define the murine CE as a powerful in vivo system to study ciliary-based cellular dynamics.

intraflagellar transport | eye development | ciliary length | microtubules

During development and tissue repair, groups of cells achieve or reconstitute highly organized patterns to form complex tissues by precisely integrating extracellular cues. How each cell converts such cues into events of cellular morphogenesis in a timely and coordinated manner is not understood (1). Primary cilia are microtubule-based antenna-like organelles protruding from the surface of vertebrate cells that mediate a number of signaling pathways during development and tissue homeostasis (2–4). The assembly, maintenance, and disassembly of cilia depend on intraflagellar transport (IFT) (5, 6). Null mutations affecting components of the IFT lead to patterning defects and midgestation lethality of the mouse embryo (7, 8). Cilia malfunction due to abnormal composition or function results in a spectrum of human syndromes referred to as ciliopathies (9–11).

As the cilium is reabsorbed before cell division, it is generally assumed that cilia appear in cells that have exited the cell cycle and entered quiescence or differentiation (12). Whereas this is true for many adult tissues, in some epithelial cells, such as the hair cells in the cochlea and the luminal cells of the mammary gland, the primary cilium regresses in the adult stage (13, 14). This led us to hypothesize that the resorption of the cilium may represent, in specific cell types, a signal of complete maturation and achievement of the normal adult cell shape and configuration in a tissue. Therefore, by controlling the assembly and disassembly of their primary cilium, cells could modulate the response to extracellular morphogenetic signals and determine their cellular architecture. Given the tridimensional nature of complex tissues, often comprising multiple cellular layers of different embryological origins, it has been difficult to follow the dynamics of ciliary assembly and disassembly in specific groups of cells and determine how these events correlate with cellular morphogenesis during development or tissue repair.

The corneal endothelium (CE), which plays an essential role in maintaining corneal transparency, offers the advantage of being organized in a 2D monolayer of hexagonal cells facing the anterior chamber of the vertebrate eye (15, 16). Because of its accessible location and simple well-defined organization, this tissue constitutes a valuable model system to study cellular morphogenesis in the context of a complex tissue during development and repair.

Although the patterning and cell density of this tissue are critical in maintaining the normal physiology of CECs, the developmental steps that control these processes remain largely unknown. Here we provide evidence that primary cilia of the mouse corneal endothelium are required to allow proper morphogenesis toward the characteristic hexagonal cell patterning of the CE during postnatal development. Furthermore, we demonstrate that primary cilia assemble only when corneal endothelial cells undergo morphogenesis during development and tissue repair but disassemble during tissue homeostasis in adult animals.

Results and Discussion

Primary Cilia Transiently Assemble on CECs from the Periphery to the Center of the CE. Several studies describe a primary cilium of unknown function on CECs of different vertebrates; however, there are discrepancies about whether all or only a subpopulation of adult CECs are ciliated (17–19). Because CECs undergo profound age-dependent morphological changes, we asked whether the presence or absence of primary cilia is associated with a specific developmental stage (or age) (20). We analyzed the CE of mice from E17.5 to adulthood. Primary cilia and basal bodies were identified by immunofluorescence using a monoclonal antibody to acetylated-α-tubulin (21), a major component of the primary cilium, and a polyclonal antibody to γ-tubulin, respectively. Cell–cell contacts were visualized with a polyclonal antibody against the tight junction protein ZO-1. Only structures stemming from basal bodies were counted as primary cilia. Primary cilia were undetectable in CE of E18.5 embryos (Fig. S1). They started to assemble as early as postnatal day 1 (1 d) but were absent in adult animals (>45–75 d; Fig. 1) In 1- to 2-d-old mice, primary cilia of about 2–3.5 μm were predominantly present on CECs located at the periphery of the cornea (Fig. 1*B*), whereas CECs present at the center of the CE only displayed a very short cilium (Fig. 1*A*). By 4 d, cilia of CECs at the center also reached a length of about 2–3 μm that persisted through 12 d, when most of the peripheral cilia began to shorten (Fig. 1 *C* and *D*). By 33–35 d, the majority of peripheral and central CECs had lost their cilia. The remaining ciliated cells presented a cilium no longer than 2 μm and were more frequent at the center than at the periphery of CE (Fig. 1 *E* and *F*). The CE of a 70-d mouse had virtually no cilia (Fig. 1*G*). Fig. 1*H* summarizes the dynamic changes of cilia length at the center and periphery of the CE at various postnatal stages.

Author contributions: C.I. designed research; A.L.B., L.P., G.L.G., J.D., and C.I. performed research; G.L.G. and J.D. contributed new reagents/analytic tools; A.L.B., G.L.G., J.D., M.M., and C.I. analyzed data; and C.I. wrote the paper.

The authors declare no conflict of interest.

*This Direct Submission article had a prearranged editor.

[1]Present address: Department of Cell Biology, State University of New York Downstate Medical Center, 450 Clarkson Avenue, Brooklyn, NY 11203.

[2]To whom correspondence may be addressed. E-mail: Marek.Mlodzik@mssm.edu or carlo.iomini@mssm.edu.

This article contains supporting information online at www.pnas.org/lookup/suppl/doi:10.1073/pnas.1016702108/-/DCSupplemental.

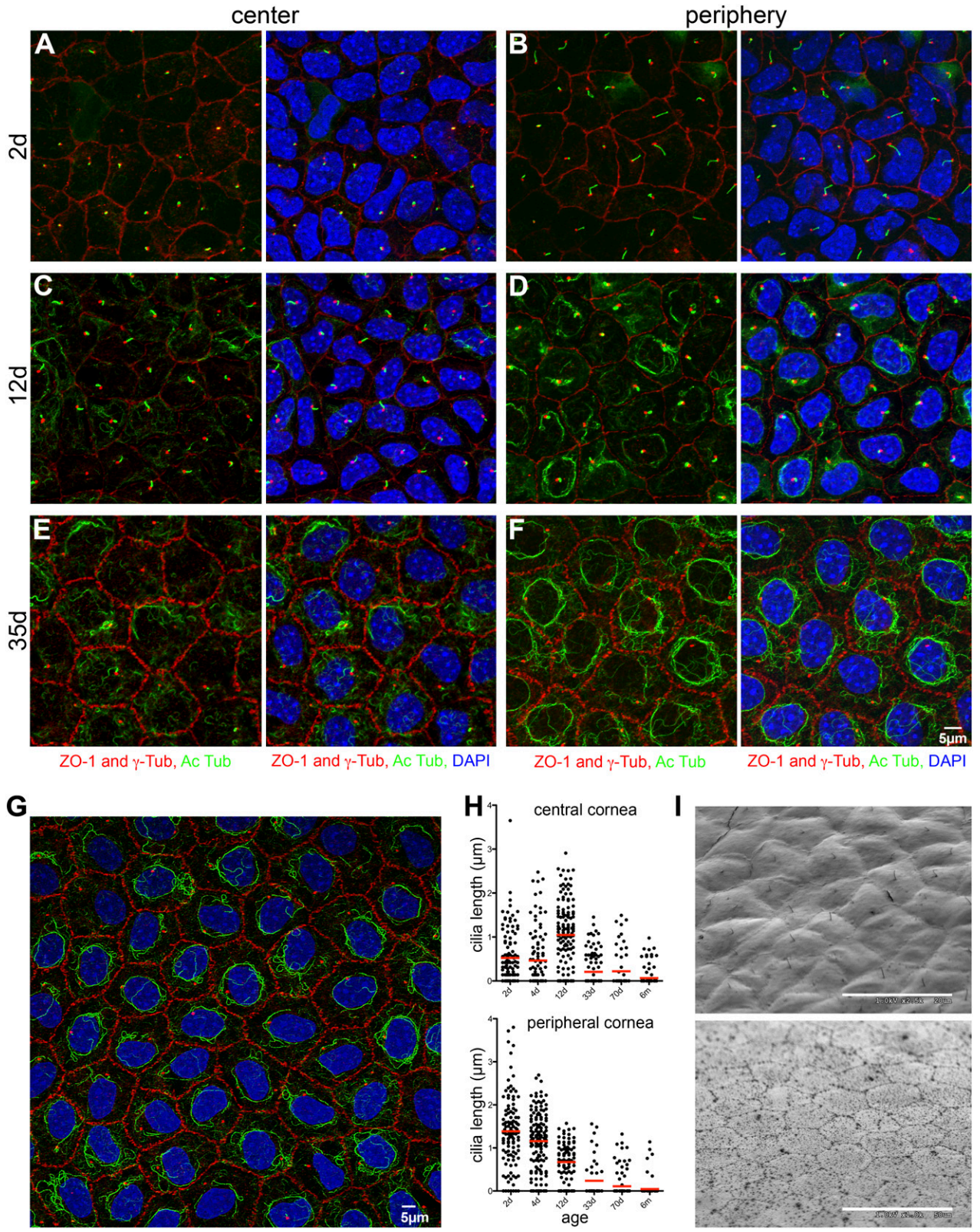

Fig. 1. Primary cilia assembly and disassembly are dynamically regulated during cellular morphogenesis and development of CE. (*A–G*) Confocal immunomicroscopy of cornea flat mount from mice at different postnatal developmental stages showing the peripheral or central areas of CE. ZO-1Ab stains cell–cell junctions and γ-tubulin the basal body at the cell center; both are shown in red, acetylated tubulin in green, and nuclei in blue. (*H*) Distribution of cilia length at the center and periphery of the cornea. On average ~100 cells at the center or at the periphery of the same cornea were counted for each age group. A similar distribution of cilia length was obtained when at least two additional corneas for each age group were analyzed. (*Y* = % and *X* = age. (*I*) SEM of CE from mice of 9 d and 7 mo reveals the presence and the absence of cilia, respectively.

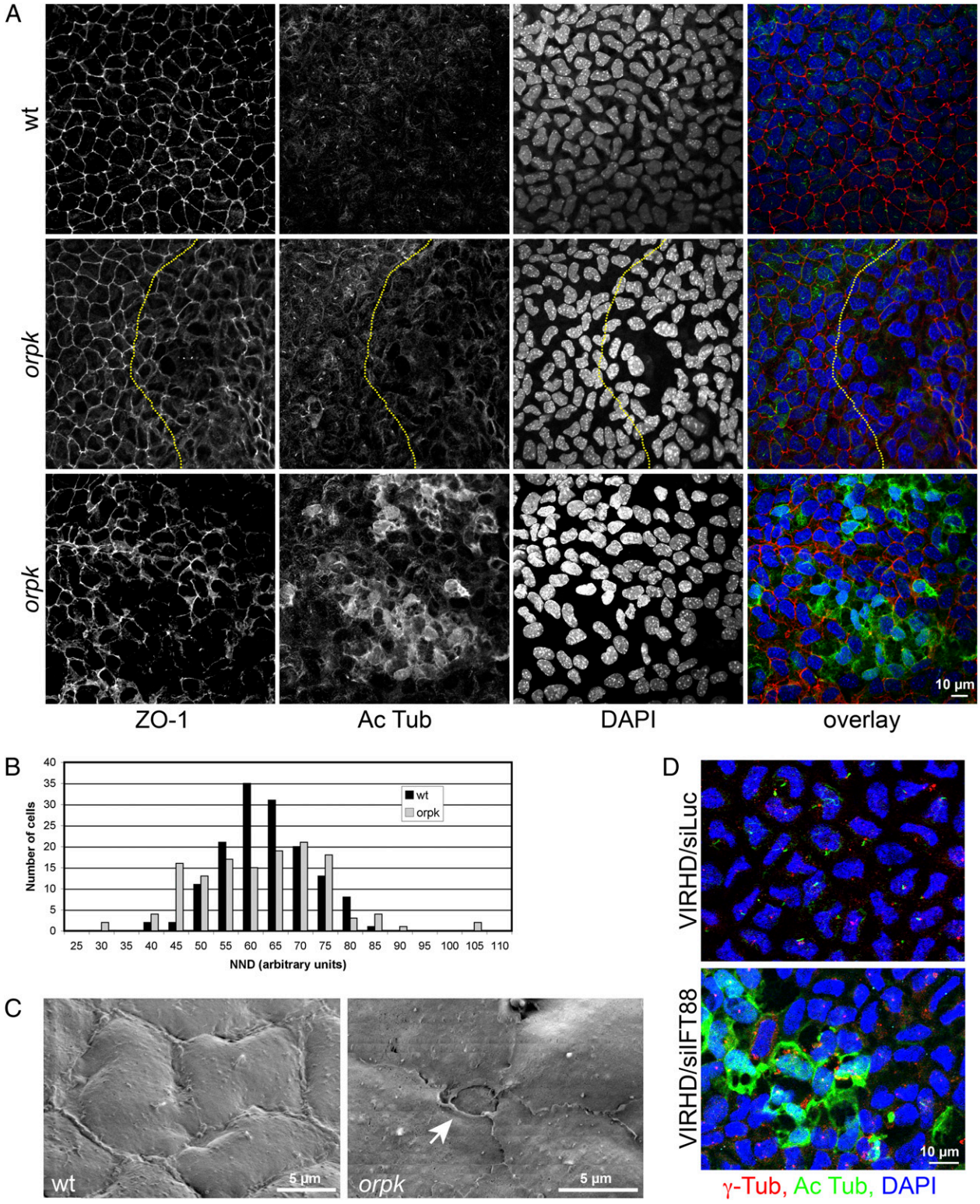

Fig. 2. Ciliary dysfunction leads to defects in CE patterning. (*A*) Confocal immunomicroscopy of 6-d-old *Tg737*^{orpk} and wild-type CE flat mount stained with indicated antibodies. (*Middle*) Only areas lacking cilia (*Right* of the dotted line) are defective in nuclei and ZO-1 distribution. (*Bottom*) Defect seems more severe and in addition to the "packaging" phenotype there is also a remarkable accumulation of cytoplasmic acetylated tubulin. (*B*) NND analysis for each nucleus was obtained by comparing the thresholded image of the nuclei in *A*, *Upper* and *Lower*). (*C*) SEM of 5-d-old wild-type and *Tg737*^{orpk} CE, *Upper* and *Lower*, respectively, Note the defect in cell–cell contact formation indicated by the arrow and blunted cilia. (*D*) Immunofluorescence of CE from 15-d-old mice injected with a lentivirus expressing the siRNA against IFT88 and a control lentivirus expressing the siRNA against luciferase. Mice were injected 6 d after birth and killed at age 15 d; the experiment was repeated twice with similar outcome. IFT88 knockdown phenocopies *Tg737*^{orpk}.

Our data suggest that assembly of primary cilia in the CE is temporally regulated, starting perinatally first on peripheral CECs and then proceeding gradually to centrally located CECs in a wave-like manner. Likewise, cilia progressively disassemble in CECs of mice older than 15 d starting from the periphery toward the center of the CE until almost complete absence in 45-d-old mice. Cilia disassembly was confirmed by analyzing CE at different postnatal time points by scanning electron microscopy (SEM) (Fig. 1*I* and Fig. S2). Interestingly, resorption of cilia coincided precisely with the progressive formation of a hexagonal CEC pattern. Early after birth, CECs appear as irregular polygons with a variable number of sides and no detectable acetylated microtubules in the cytoplasm. By day 30–35, CECs achieved a hexagonal shape with characteristic bundles of acetylated microtubules around the nucleus (Fig. 1 *A*–*F*).

CE Cellular Pattern Is Altered in *Tg737*^{orpk} Mice, a Hypomorphic Allele of IFT88. The tight correlation between shape changes, cytoskeletal remodeling, and cilia assembly and disassembly in CECs during postnatal development led us to hypothesize that the cilium of CECs controls CE patterning. Null mutations that completely abolish cilia lead to midgestation lethality, before the CE layer is established (22). The IFT88 protein is a component of the IFT, the bidirectional movement of particles between the tip and the base of the cilium required for cilia assembly and maintenance first described in *Chlamydomonas* (23). The hypomorphic *Ift88* allele in the *Tg737*^{orpk} mouse leads to cilia that are stunted and malformed, but not completely abolished, thus allowing these homozygous mutants to survive within the weaning period (24). In contrast, mice that are heterozygous for this mutation appear indistinguishable from wild-type littermates (25). To determine CE patterning in tissues with aberrant cilia, we isolated corneas from *Tg737*^{orpk} mice ($n = 5$) and wild-type or heterozygous littermates at different postnatal developmental ages between 4 d and 19 d. To visualize the cell contacts, primary cilia, and nuclei of CECs, flat mounted corneas were stained with antibodies against ZO-1, acetylated tubulin, and DAPI. Cilia length and distribution differed significantly between *Tg737*^{orpk} homozygotes compared with control littermates. Whereas some areas of CE in the corneas of *Tg737*^{orpk} homozygotes exhibited cilia of fairly normal length, other areas presented short or absent cilia (Fig. 2*A*, *Middle* and *Bottom*, respectively). Within CE areas with defective cilia, CECs displayed a disorganized cellular pattern, ZO-1 mislocalization, and cytoplasmic accumulation of acetylated tubulin. SEM micrographs occasionally showed incomplete cellular junction formation between CECs with short cilia in *Tg737*^{orpk} mice (Fig. 2*C*). In contrast, all CECs in wild-type or heterozygous littermates showed normal cilia and cellular distribution (Fig. 2*A*, *Top*). The patterning of the CECs in mutant mice was compared with that in wild-type using an image analysis approach and quantified (Fig. 2*B*). Notice that the nearest neighbor distance (NND) distribution of the CEC nuclei in *Tg737*^{orpk} was much wider than that of wild-type controls. To determine whether the aberrant spacing of the nuclei in the CE of *Tg737*^{orpk} was a consequence of cell death we performed TUNEL analysis on developing CE. No TUNEL-positive cells were detected on CE of 4-d *Tg737*^{orpk} and wild-type littermate mice (Fig. S3). In addition, the CEC density is similar in both wild-type and mutant strains as assessed in 6-d old mice [wild type, 154 cells/0.02 mm^2 ($n = 3$) and *Tg737*^{orpk}, 151.3 cells/0.02 mm^2 ($n = 3$)]. These results suggest that apoptosis does not account for CE patterning defects detected in the *Tg737*^{orpk} mouse. Next, we tested whether the abnormal tissue patterning in *Tg737*^{orpk} CE is due to defective morphology of individual CECs. We measured the area and the "shape factor" of the polygons identified by the cell–cell contacts in the CE labeled by the ZO-1 antibody in both strains. The distribution of the polygonal areas in the CE of 6-d *Tg737*^{orpk} mice was wider than that of wild-type littermates and the means of the CEC shape factor was 0.64 and 0.71 in the *Tg737*^{orpk} and wild-type mice, respectively, implying an intrinsic defect of the overall architecture of the CECs in the *Tg737*^{orpk} mice (Fig. S4). Taken together, these results suggest a critical role of IFT88 in the cytoskeletal remodeling and cellular morphogenesis of CECs required for tissue patterning in the developing CE.

Given the nonconditional nature of the *Tg737*^{orpk} mutation, we cannot however exclude that the CE phenotype of newborn *Tg737*^{orpk} mice resulted from defective interactions between neural crest progenitors of CECs and other ciliated cells early in development or from a role of IFT88 in neural crest cell migration similar to that described for other basal body and ciliary proteins (26). To exclude these possibilities, we knocked down IFT88 expression in CECs in vivo using a lentiviral-mediated RNAi approach.

Lentiviral-Mediated IFT88RNAi Phenocopies *Tg737*^{orpk} Defects in CE. As previously shown, primary cilia persist on mouse CECs for about 4 wk after birth. During this time, CECs undergo morphogenesis to acquire a hexagonal shape (Fig. 1). To specifically inactivate IFT88 in the CE, we injected the anterior chamber of 5- to 6-d old mice with 2 μL of VIRHD/E/siLuc or VIRHD/E/siIFT88 lentivectors expressing an siRNA hairpin against luciferase (control) or the murine IFT88 gene, respectively (27). Transduction rates in vivo and cell-type specificity were monitored by injecting the VVPW/H2B-cherry lentivirus expressing cherry-tagged histone H2B under the constitutive CMV promoter. Virtually all CECs, but no other corneal cell types, expressed H2B-cherry in the nucleus (Fig. S5).

Corneas were isolated 5–7 d after injection and analyzed by immunofluorescence. Several areas of the CE from eyes injected with VIRHD/E/siIFT88 showed defects similar to those affecting the CE of *Tg737*^{orpk} mice: absent or shortened cilia and corresponding abnormal patterning of CECs (Fig. 2*D*). In contrast, none of these defects were observed in CEs of mice injected with the control lentivector VIRHD/E/siLuc. These results indicate that primary cilia play an instructive role in determining the normal patterning of the CE during postnatal development.

Primary Cilia Assemble During in Vivo CE Repair in Adult Mice. We next asked whether components of the IFT machinery that are required for ciliary assembly were still present in CECs of adult mice. Staining with antibodies specific for IFT72/74 (also known as CMG-1Ab) (28) and IFT88 was detected along the cilium and at the basal body of CECs in 4-d-old mice and at the basal body of CECs in 7-mo-old mice (Fig. 3 and Fig. S6). Therefore, IFT components persist at the basal body of CECs in adult mice,

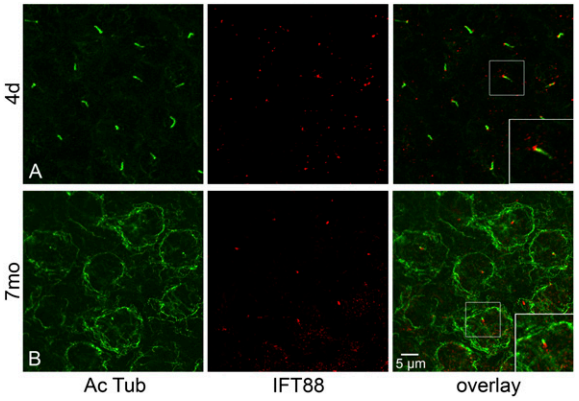

Fig. 3. IFT proteins in CE of young and adult mice. Immunofluorescence of flat mount of CE from 4-d- and 7-mo-old mouse stained with acetylated tubulin Ab (green) and IFT88Ab (red).

suggesting that CECs maintain the ability to reassemble a primary cilium.

To further address the notion that cilia orchestrate cellular morphogenesis of CECs, we tested the hypothesis that the cilium reassembles when cellular morphogenesis is reinduced in the CE of adult mice by wounding. As CECs show little or no proliferation during wound repair, they stretch and migrate in a direction perpendicular to the wound to cover the exposed Descemet's membrane, losing their normal hexagonal shape (29). Typically, after 48 h, a wound of about 3 mm is repaired by a complete layer of enlarged CECs, characterized by an irregular shape, which persists for several months (30). To investigate a possible role of primary cilia in endothelial repair in vivo, we produced a linear endothelial wound in the CE of adult mice. The wound was generated by gently scraping cells with a 10.0 suture surgical needle inserted into the anterior chamber of the eye of 5- to 6-mo-old mice and passed across the CE. After 18 h and 30 h of healing time, mice were killed and corneas were removed and analyzed. Cilia of about 2–3 μm were detected on CECs near the wound (4–5 cell rows) as early as 18 h after wounding (Fig. 4*A*). Although newly ciliated CECs within 4–5 cell rows next to the wound maintained a shape close to a hexagon, the perinuclear bundles of acetylated microtubules were disorganized or absent and the basal bodies localized at the median of the cell (Fig. 4 *A* and *D*). In corneas isolated 30-h postwounding, CECs neighboring the wound still showed a primary cilium and lacked cytoplasmic acetylated microtubules. In addition, their shape was elongated in the axis perpendicular to the wound and the basal bodies polarized to the cell side closer to the wound (Fig. 4 *B* and *D*). In contrast, CECs away from the

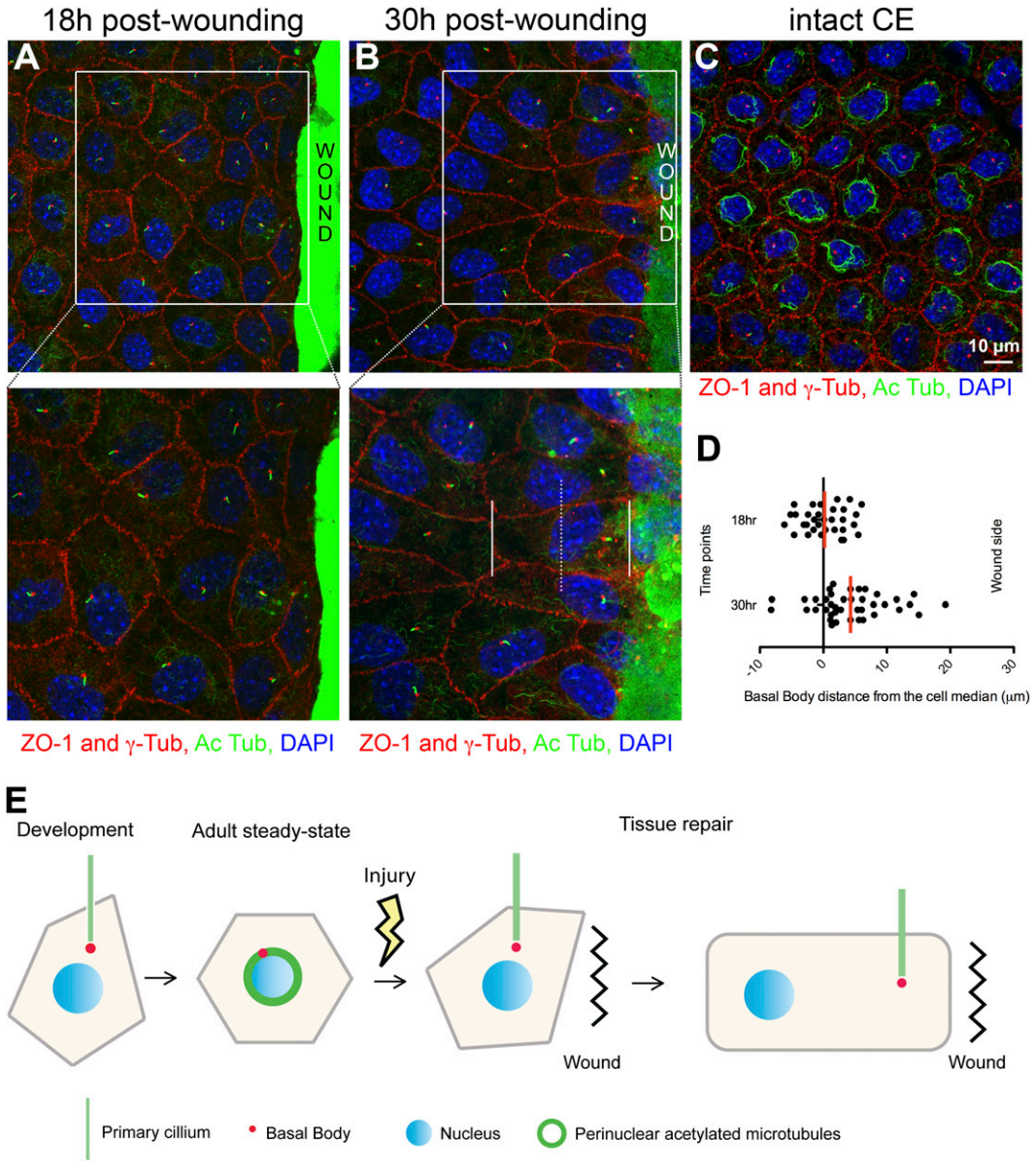

Fig. 4. Cilia assembly, cellular remodeling, and basal body polarization of CECs during CE repair. (*A* and *B*) Wounded area of CE 18 h and 30 h after in vivo recovery. Corneas were dissected from 3-mo-old mice. (*C*) Intact area of the same CE shown in *B*, located ~150–200 cell rows away from the wounded area. (*D*) Basal body distance from the cell median, measured as shown by the dotted line in *B*, *Bottom*. (*E*) Model of the cilia dynamics during cellular morphogenesis in development and repair (see text). Acetylated tubulin is shown in green, ZO-1 and γ-tubulin in red, DAPI in blue. Data corroborating the reorientation of the basal body were obtained in additional independent experiments and are shown in Fig. S7.

wounded area (~150–200 cell rows) remained aciliated and maintained their hexagonal shape, the perinuclear bundle of acetylated microtubules, and the basal bodies localized near the cell center (Fig. 4*C*).

Taken together, our data indicate that cilia are present on CECs during events of cellular remodeling, occurring in development or tissue repair of the CE, but disassemble during steady state in normal adult CE (Fig. 4*E*). In support of this idea, we have shown that ciliary dysfunction leads to defective patterning of CE during postnatal development. Intriguingly, findings in other tissues support similar conclusions. The kinocilium, the primary cilium found in inner ear hair cells, is required for proper development of the organ of Corti but it is reabsorbed about 10 d after birth. However, following trauma, hair cells from differentiated cochlea reassemble their kinocilia regardless of age, as shown in in vivo and ex vivo experiments in mice and rabbits (31, 32). During development and repair, inner ear hair cells undergo morphogenesis and show intense remodeling of the microtubular and actin cytoskeleton, and the kinocilium controls the localization of the basal bodies within hair cells (31, 33). In addition, primary cilia in adult kidney cells not only act as flow sensors, but may also be involved in epithelial differentiation during renal injury and repair. For example in mice, tubular damage causes an increase and a subsequent regression of cilium length during renal repair (34). Moreover *foxj1a*, the transcriptional regulator of cilia genes, is rapidly induced in response to epithelial stretch or injury (35). Thus, in general, the reassembly of primary cilia in adult tissues seems to represent a very early response to an injury. Interestingly, *Tg737*^{orpk} mice show defects in wound closure (36). Recent studies have shown that spatial constraint and actin cytoskeleton remodeling can control cilia elongation and resorption (37). It is tempting to speculate that mechanical forces generated during tissue patterning and disrupted by an injury can modulate the cellular response to cilia-mediated signaling by controlling primary cilia dynamics. Identifying the cues and the mechanism promoting ciliary assembly upon tissue damage, and the signaling pathways mediated by this organelle during the healing process, could improve our understanding of how to treat injuries. Due to its simple organization as a monolayer facing the ocular anterior chamber and its accessibility to lentivector-mediated gene transfer that can be monitored in vivo by confocal microscopy, the CE provides a unique valuable model system to study the dynamic properties and function(s) of primary cilia in cellular morphogenesis during tissue development and repair.

Materials and Methods

The mouse strains and oligonucleotide sequences used in this study as well as a detailed description of lentiviral production, microscopy and morphometric analysis, and in vivo wound healing experiments are provided in *SI Materials and Methods*.

ACKNOWLEDGMENTS. We thank Brad Yoder (Alabama University), Beth Zavilowitz, and Lisa Satlin [Mount Sinai School of Medicine (MSSM)] for providing and breeding *Tg737*^{orpk} mice, and all members of the Mlodzik laboratory for helpful discussion. We are grateful to Dr. Ron Gordon and Heather Bell at the Mount Sinai Electron Microscopy Facility for helping with SEM analysis, Lizhen Ren for technical support, and Susanna Franks for assisting with the illustrations. Confocal laser scanning microscopy was performed at the MSSM-Microscopy Shared Resources Facility, supported with funding from National Institutes of Health (NIH)-National Cancer Institute Shared Resources Grant 5R24 CA095823-04, National Science Foundation Major Research Instrumentation Grant DBI-9724504, and NIH Shared Instrumentation Grant 1 S10 RR0 9145-01. This research was supported by NIH Grants HD058039 (to C.I.), DK78231 (to G.L.G.), EY014592 (to M.M.), and Department of Defense Grant W81XWH-09-1-0269 (to G.L.G.). C.I. is a Young Investigator of the National Kidney Foundation (YIB1110).

1. Davies JA (2005) *Mechanisms of Morphogenesis* (Academic, London).
2. Berbari NF, O'Connor AK, Haycraft CJ, Yoder BK (2009) The primary cilium as a complex signaling center. *Curr Biol* 19:R526–R535.
3. Christensen ST, Pedersen LB, Schneider L, Satir P (2007) Sensory cilia and integration of signal transduction in human health and disease. *Traffic* 8:97–109.
4. Pazour GJ, Witman GB (2003) The vertebrate primary cilium is a sensory organelle. *Curr Opin Cell Biol* 15:105–110.
5. Pan J, Snell WJ (2005) Chlamydomonas shortens its flagella by activating axonemal disassembly, stimulating IFT particle trafficking, and blocking anterograde cargo loading. *Dev Cell* 9:431–438.
6. Rosenbaum JL, Witman GB (2002) Intraflagellar transport. *Nat Rev Mol Cell Biol* 3: 813–825.
7. Sharma N, Berbari NF, Yoder BK (2008) Ciliary dysfunction in developmental abnormalities and diseases. *Curr Top Dev Biol* 85:371–427.
8. Goetz SC, Anderson KV (2010) The primary cilium: A signalling centre during vertebrate development. *Nat Rev Genet* 11:331–344.
9. Badano JL, Mitsuma N, Beales PL, Katsanis N (2006) The ciliopathies: An emerging class of human genetic disorders. *Annu Rev Genomics Hum Genet* 7:125–148.
10. Marshall WF (2008) The cell biological basis of ciliary disease. *J Cell Biol* 180: 17–21.
11. Zariwala MA, Knowles MR, Omran H (2007) Genetic defects in ciliary structure and function. *Annu Rev Physiol* 69:423–450.
12. Veland IR, Awan A, Pedersen LB, Yoder BK, Christensen ST (2009) Primary cilia and signaling pathways in mammalian development, health and disease. *Nephron, Physiol* 111:39–53.
13. Kikuchi K, Hilding D (1965) The development of the organ of Corti in the mouse. *Acta Otolaryngol* 60:207–222.
14. McDermott KM, Liu BY, Tlsty TD, Pazour GJ (2010) Primary cilia regulate branching morphogenesis during mammary gland development. *Curr Biol* 20:731–737.
15. Cvekl A, Tamm ER (2004) Anterior eye development and ocular mesenchyme: New insights from mouse models and human diseases. *Bioessays* 26:374–386.
16. Hogan MJ, Alvarado JA, Weddell JE (1971) *Histology of the Human Eye* (Saunders, Philadelphia).
17. Doughty MJ (2004) Influence of initial fixation protocol on the appearance of primary cilia on the rabbit corneal endothelial cell apical surface as assessed by scanning electron microscopy. *Cell Biol Int* 28:131–137.
18. Collin SP, Collin HB (1998) A comparative study of the corneal endothelium in vertebrates. *Clin Exp Optom* 81:245–254.
19. Svedbergh B, Bill A (1972) Scanning electron microscopic studies of the corneal endothelium in man and monkeys. *Acta Ophthalmol (Copenh)* 50:321–336.
20. Murphy C, Alvarado J, Juster R, Maglio M (1984) Prenatal and postnatal cellularity of the human corneal endothelium. A quantitative histologic study. *Invest Ophthalmol Vis Sci* 25:312–322.
21. Piperno G, LeDizet M, Chang XJ (1987) Microtubules containing acetylated alpha-tubulin in mammalian cells in culture. *J Cell Biol* 104:289–302.
22. Saika S, et al. (2001) TGFbeta2 in corneal morphogenesis during mouse embryonic development. *Dev Biol* 240:419–432.
23. Pazour GJ, et al. (2000) *Chlamydomonas IFT88* and its mouse homologue, polycystic kidney disease gene *tg737*, are required for assembly of cilia and flagella. *J Cell Biol* 151:709–718.
24. Lehman JM, et al. (2008) The Oak Ridge Polycystic Kidney mouse: Modeling ciliopathies of mice and men. *Dev Dyn* 237:1960–1971.
25. Moyer JH, et al. (1994) Candidate gene associated with a mutation causing recessive polycystic kidney disease in mice. *Science* 264:1329–1333.
26. Tobin JL, et al. (2008) Inhibition of neural crest migration underlies craniofacial dysmorphology and Hirschsprung's disease in Bardet-Biedl syndrome. *Proc Natl Acad Sci USA* 105:6714–6719.
27. Battini L, et al. (2006) Stable knockdown of polycystin-1 confers integrin-alpha2beta1-mediated anoikis resistance. *J Am Soc Nephrol* 17:3049–3058.
28. Iomini C, Tejada K, Mo W, Vaananen H, Piperno G (2004) Primary cilia of human endothelial cells disassemble under laminar shear stress. *J Cell Biol* 164:811–817.
29. Joyce NC (2003) Proliferative capacity of the corneal endothelium. *Prog Retin Eye Res* 22:359–389.
30. Tuft SJ, Williams KA, Coster DJ (1986) Endothelial repair in the rat cornea. *Invest Ophthalmol Vis Sci* 27:1199–1204.
31. Sobkowicz HM, Slapnick SM, August BK (1995) The kinocilium of auditory hair cells and evidence for its morphogenetic role during the regeneration of stereocilia and cuticular plates. *J Neurocytol* 24:633–653.
32. Engström B, Flock A, Borg E (1983) Ultrastructural studies of stereocilia in noise-exposed rabbits. *Hear Res* 12:251–264.
33. Jones C, et al. (2008) Ciliary proteins link basal body polarization to planar cell polarity regulation. *Nat Genet* 40:69–77.
34. Verghese E, et al. (2009) Renal primary cilia lengthen after acute tubular necrosis. *J Am Soc Nephrol* 20:2147–2153.
35. Hellman NE, et al. (2010) The zebrafish foxj1a transcription factor regulates cilia function in response to injury and epithelial stretch. *Proc Natl Acad Sci USA* 107: 18499–18504.
36. Schneider L, et al. (2010) Directional cell migration and chemotaxis in wound healing response to PDGF-AA are coordinated by the primary cilium in fibroblasts. *Cell Physiol Biochem* 25:279–292.
37. Pitaval A, Tseng Q, Bornens M, Théry M (2010) Cell shape and contractility regulate ciliogenesis in cell cycle-arrested cells. *J Cell Biol* 191:303–312.